

MECHANICAL DESIGN FOR AN X-RAY DIFFRACTION MICROPROBE AT THE ADVANCED PHOTON SOURCE*

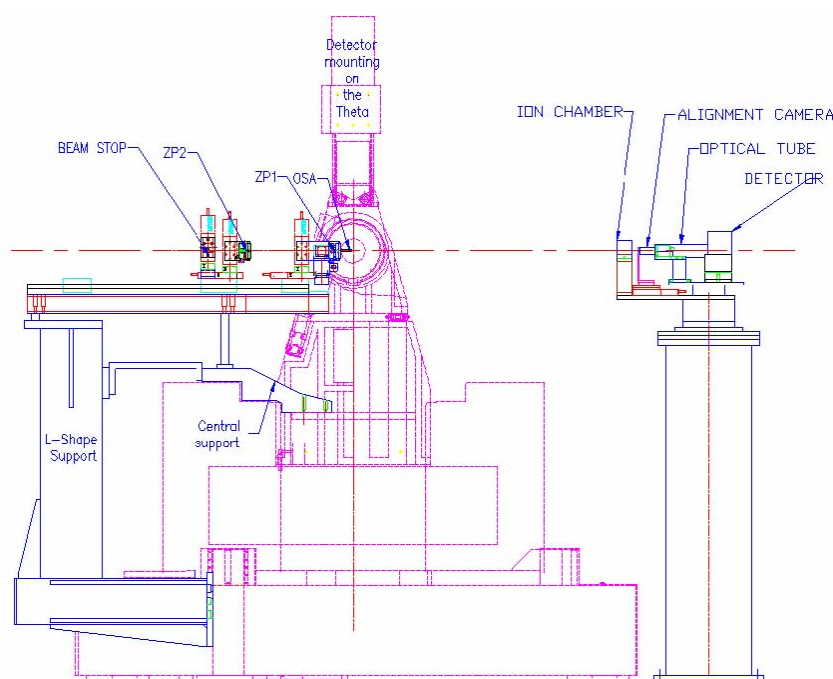
S. Xu, Z. Cai, and B. Lai

Argonne National Laboratory-9700 S. Cass Avenue Argonne- IL 60439, U. S. A.

Abstract

An x-ray diffraction microprobe has been constructed and commissioned at the 2-ID-D beamline of the Advanced Photon Source. This new instrument is capable of high-resolution spatial mapping of crystallographic phase, lattice strain, and lattice distortion with energies from 6 to 20 keV. The mechanical design for the x-ray diffraction microprobe involves integrating a hard x-ray Fresnel zone-plate-based microprobe into a six-circle kappa diffractometer, while reducing as much as possible the mechanical interference between the microprobe and the diffractometer. In-depth vibration analysis were performed on various parts of the diffractometer to ensure that the spatial resolution would not be compromised, which was subsequently confirmed by knife edge measurements indicating focal spot size of < 200 nm. An energy dispersive detector was incorporated for sample alignment and analysis using x-ray fluorescence. Alignment mechanism for stacked zone plate was also included to provide higher focusing efficiency with x-ray energy up to 30 keV. The x-ray diffraction microprobe has been applied to studies of the microstructures of bicrystal-supported magnetoresistive films, crystallographic phases in zirconium oxide layers, strain induced by various microstructures, and structures in nanowires.

A zone-plate-based hard x-ray microprobe (HXRM) has been implemented for a wide range of x-ray experimental techniques at station 2-ID-D of the Advanced Photon Source (APS) at Argonne National Laboratory.¹ We report here the mechanical integration of a HXRM with a six-circle diffractometer for microdiffraction experiments. The kappa geometry of the diffractometer was selected to accommodate the needs of the HXRM for the space near the specimen and, thus, to provide a wider access to reciprocal space. diffractometer.



The diffractometer is an N6050-K1 goniometer made by Newport Micro-Controle, which contains four sample circles and two detector circles. The four sample circles are in the kappa geometry with a 50° angle between the kappa and omega axes. The kappa geometry of the diffractometer was selected to accommodate the needs of the HXRM for the space near the specimen and to provide a wider access to reciprocal space. The on-axis encoders and the closed-loop servo-driver systems provide angular resolution of 0.0001° for sample and detector circles and 0.00025° for circles that carry the sample-circle assembly and detector-arm assembly.



Figure 2: Overview of the hard x-ray microprobe, detector, and the diffractometer in the 2-ID-D station of APS. The diffractometer is N6050-K1 goniometer from (Newport) Micro-controlle with four sample circles on Phi, Kappa, Omega, and Mu axes, and two detector circles on Theta and Nu axes.

The stability of the supporting structure for the HXRM assembly is critical for achieving high performance. As shown in Figs. 1-3, the table top for the HXRM is supported at one end directly on the central table of the diffractometer, and the other end is supported by a L-shape weldment of structural steel reinforced with welded steel webs along both vertical and horizontal directions.² Both the central table and the weldment are mounted directly on the diffractometer's granite base.



Fig. 3: Close-up view of hard X-ray microprobe, detector, and sample mounting system. The microprobe is mounted on carriages of Thomson linear guide which mounted on a special optical table. The detector is mounted on the Theta axis arm. The four sample circles are in the kappa geometry with a 50° angle between the kappa and omega axes.

We have designed and constructed a vibration-damping structure for the diffractometer supporting system, similar to the one that was installed in a scanning x-ray fluorescence microprobe for isolation of vibration from the floor. Three support blocks replaced previous mechanical stages for the granite base. The bottom of the block was machined with a flatness of better than 0.002 mm to form a base for a vibration-damping sandwich structure. The vibration-damping sandwich structure, $\phi 180$ mm in size, consists of a leg base and a steel mounting plate joined by a layer of 150- μ m pressure-sensitive adhesive film of proprietary acrylic materials (Anatrol 217 in this case). The relative motion between the leg base and the steel mounting plate induces large cyclic shear strains in the film resulting in substantial energy dissipation. Vibration measurements using seismic accelerometers indicate no amplification of the vibration, within the detection sensitivity of 5 nm in amplitude, is generated because of the supporting structure.

The mechanics of the HXRM include two zone plate assemblies for short-focal-length (100 mm) and long-focal-length (400 mm) zone plates, a beam central stop assembly, and an order-sorting-aperture assembly (Fig. 4). Zone-plate assembly contains three orthogonal translations for positioning of the zone plate against incident beam transversely and focal distance longitudinally. The two zone plates provide

high and moderate focusing power. In order to further improve focusing efficiency and extend the zone-plate microfocusing capability into higher energy,⁵ each zone-plate assembly is capable of stacking two identical zone plates (Fig. 5) within focal depth (100 μm for 100 mm zone plate) of the zone plate longitudinally and within the outmost zone width (0.1 μm for 100 mm zone plate) of the zone plate transversely. The stacking of the zone plates equivalently doubles the thickness of a single zone plate. As such, two additional orthogonal translations in the transverse plane need to be added for the second stacking zone plate. The beam-central-stop and order-sorting-aperture assemblies contain two orthogonal translations in the plane transverse to the incident beam. The central stop prevents undiffracted x-rays from reaching the specimen. The focused beam is filtered through an order-sorting aperture to prevent unwanted diffraction orders from reaching the specimen.

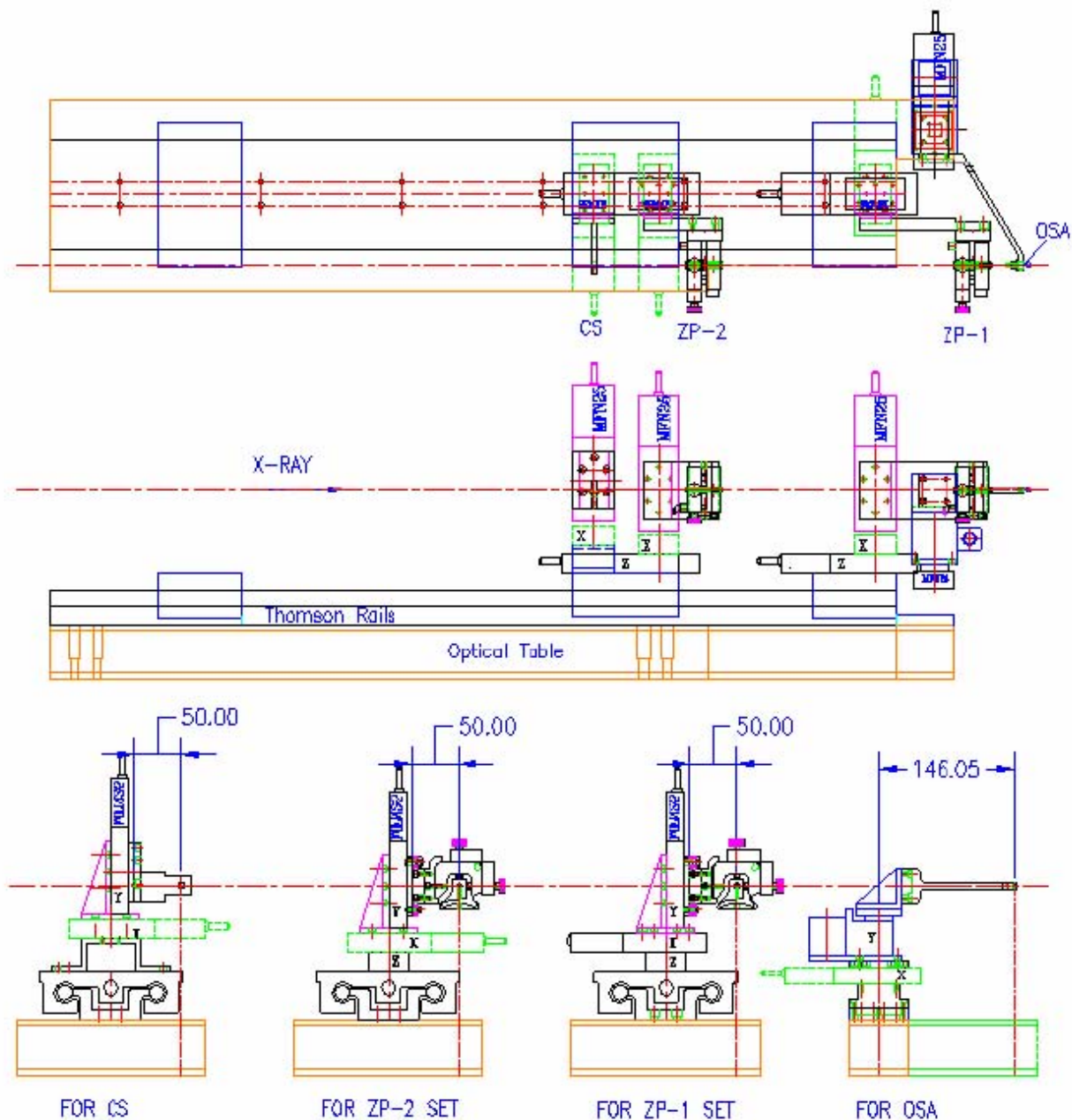


Fig. 4: Layout of the hard X-Ray microprobe. All optical components with xyz motorized stages for focal length adjustment and positioning in the transverse plane.

The criteria for two zone plates to be aligned have been established by looking at the interference patterns of x-rays focused by individual zone plates in real-time. ³ Fig. 5 shown each zone plate is positioned with flexure stage (New Focus). Two of these stages are mounted parallel to each other on an adapting plate. The zone plates are glued with nail polish onto a cylindrical carrier, which can be moved longitudinally within flexure stage to minimize their proximity. One flexure is pre-aligned mechanically. The second zone plate and the central stop are aligned with respect to the first zone plate using piezo-micrometer actuators.

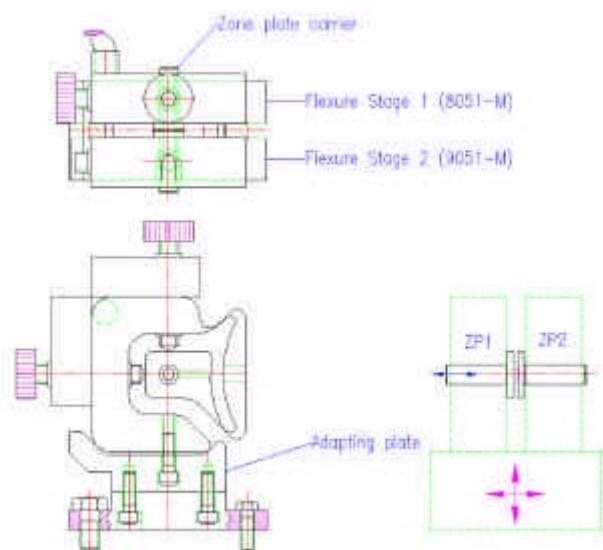


Fig. 5: The stages are placed on an adapting plate, which maintains parallel alignment between two zone plates in very close proximity. The zone plates are glued on small aluminum carriers and inserted into the central hole in the stage. The carrier can be moved longitudinally to change the separation between the two zone plates.

Fig. 6 shows a CCD camera and a CCD detector are installed at about 1.1 meter downstream from the center of the diffractometer for aligning the x-ray microprobe and specimens. X-ray image is transformed to an image of visible light at the front surface of either a CdWO₄ scintillation crystal for higher conversion efficiency or a YAG:Ce/YAG for higher resolution. The visible light image is captured by the CCD camera or the CCD detector through an optical imaging system. The both CCD devices are carried by a vertical stage and a horizontal stage for positioning and switching between them. The both CdWO₄ scintillation crystal and the doped YAG crystal are carried by a translation stage along the beam direction for focusing alignment of the optical imaging system. The two crystals can be switched with a manual stage.

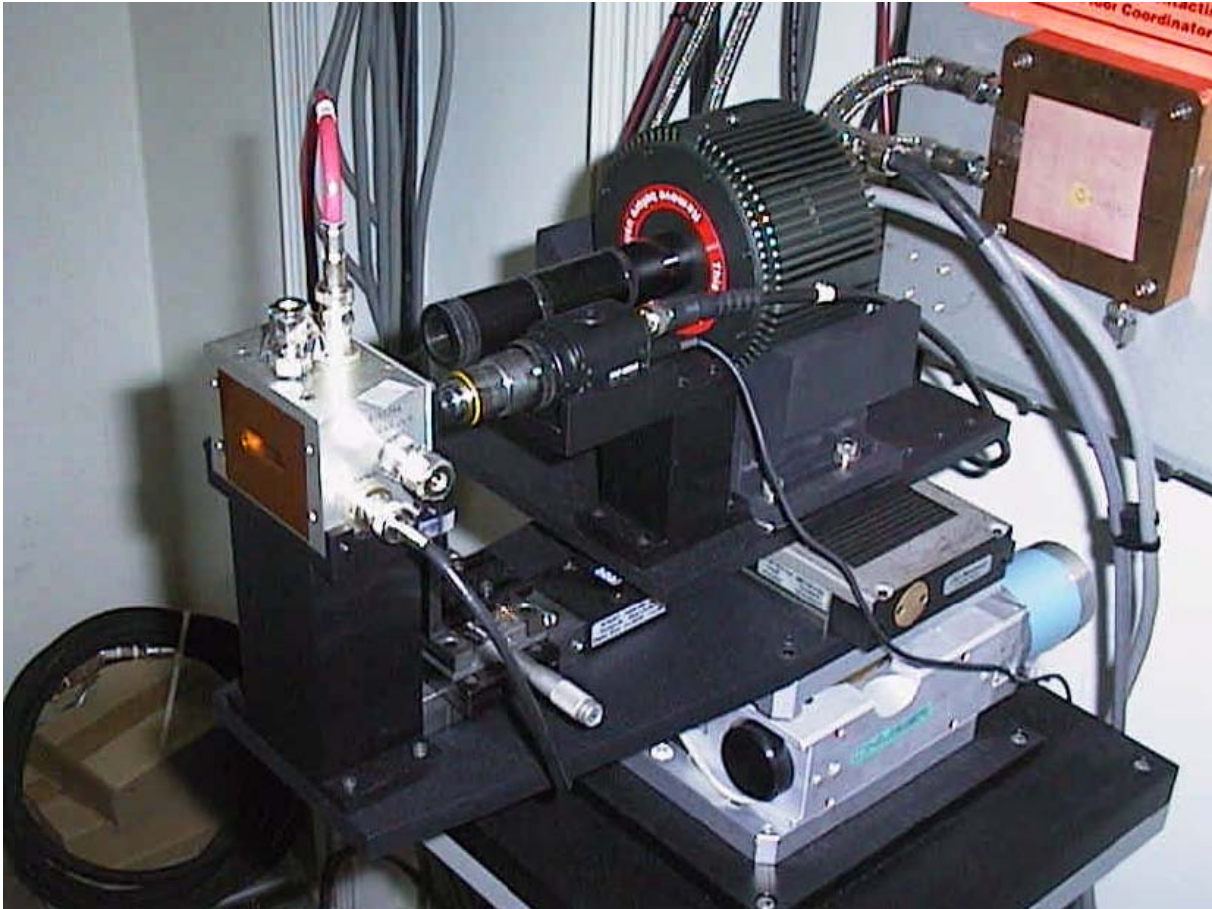


Fig. 6: Close-up view of the alignment system. A video camera and a CCD camera were mounted on X-Y stages to align to the x-ray beam. A scintillation screen was mounted on a Z stage upstream of the camera for focusing onto the cameras.

In Fig. 7 we display the patterns obtained with different extents of the displacement between the two zone plates recorded with a CdWO₄ scintillation screen, a microscope objective, and a CCD camera placed downstream of the focal spot (see Fig. 6). The first picture A shows prior to alignment, with vertical misalignment of several μm . Picture B shows reduced vertical misalignment and have some horizontal misalignment. The picture C shows reduced vertical misalignment to a few zones and picture D shows both zone plates aligned. Decreasing the spatial frequency of the interference feature in the pattern indicates a good trend in the alignment, and the spatial frequency becomes zero as the two zone plates are perfectly aligned. However, one has to avoid the other extreme where the two zone plates are completely off aligned and no interference would take place.

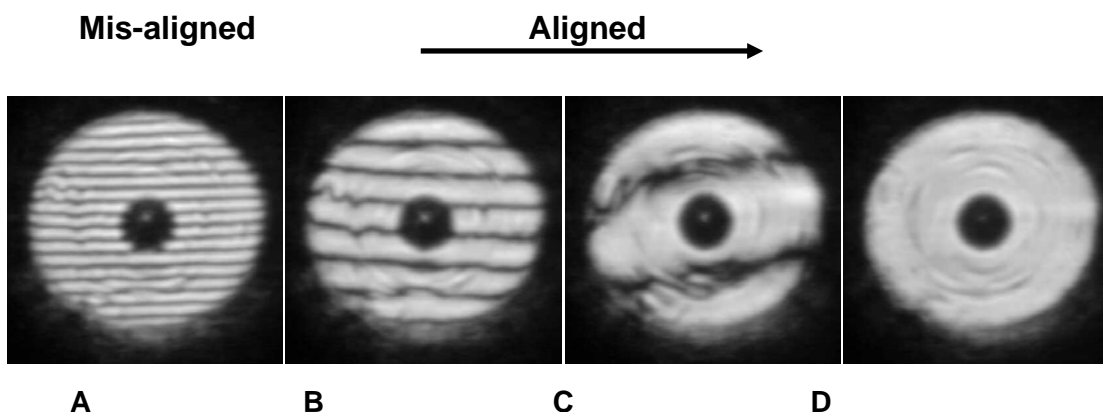


Fig. 7: Images of interference patterns formed from X-rays focused with two zone plates, recorded downstream from the focal plate. Image sequence shows the alignment procedure of two stacked zone plates. The dark spot in the center is due to the beam stop.

The measurement of the apparent focal spot size obtained from a 100 mm zone plate at 10 keV was performed by scanning a tin oxide nanobelt of size less than 100 nm across the focal spot and measuring the intensity of the Sn L-line fluorescence at every position of the nanobelt in the focal spot. The sample stage assembly that carries the nanobelt was mounted on sample circles of the diffractometer. As shown in Fig. 8, a FWHM spot size along horizontal direction of less than 190 nm was obtained. The measured spot size is a convolution of the true spot size and the instability of the relative position between the optical axis of the HXRM and the nanobelt held by sample assemble.

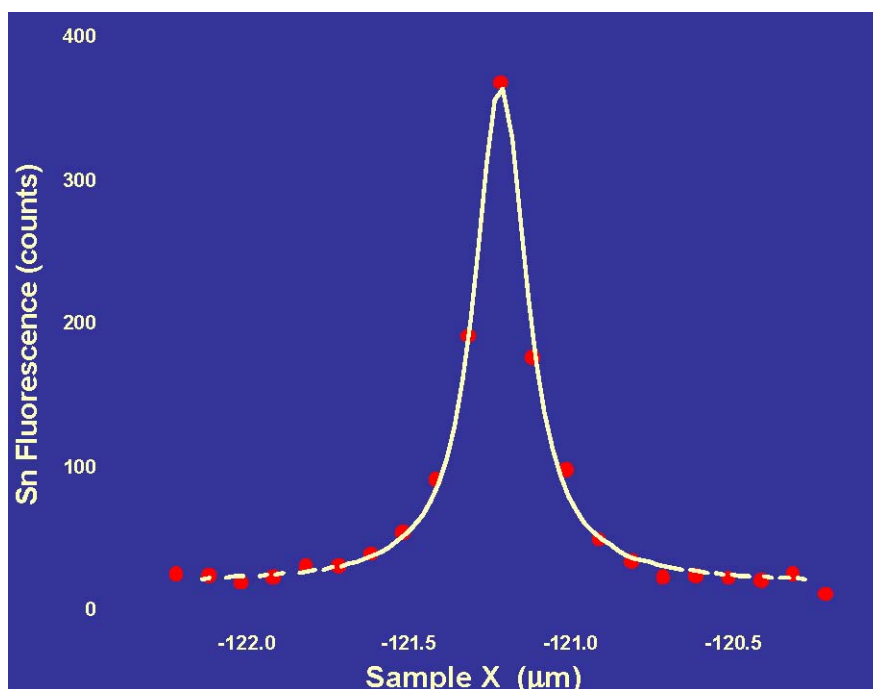


Fig. 8: Measured Sn X-Ray fluorescence profile while X-Ray beam is scanned across a 100-nm belt. The effective focal spot size is less than 190 nm.

* This work was supported by the U.S. Department of Energy, Office of Science, Basic Energy Sciences, under Contract No. W-31-109-ENG-38.

References:

- [1] Z. Cai, B. Lai, W. Yun, P. Ilinski, D. Legnini, J. Maser, W. Rodrigues, in *X-ray Microscopy*, Proceedings of the Sixth International Conference, Vol. 507, W. Meyer-Ilse, T. Warwick, and D. Attwood, eds., (AIP, 2000) pp. 472-477.
- [2] J. Libera, Z. Cai, B. Lai, and S. Xu, *Rev. Sci. Instrum.* **73**, 1506 (2002).
- [3] S. Xu, B. Lai, Z. Cai, and D. Shu, *Rev. Sci. Instrum.* **73**, 1599 (2002).
- [4] D. Mangra, S. Sharma, and C. Doose.:” Performance of the Vibration Damping Pads in the APS Storage Ring” 1# International Workshop on Mechanical Engineering Design of Synchrotron Radiation Equipment and Instrumentation. July13-14, Switzerland.
- [5] J. Maser, B. Lai, W. Yun, S. D. Shastri, Z. Cai, W. Rodrigues, S. Xu, *Proceedings of SPIE* Vol. 4783 (2002), pp. 74-81.